CRYSTAL GROWTH & DESIGN

Article

Cite This: *Cryst. Growth Des.* 2018, 18, 4365−4371

pubs.acs.org/crystal

Mixed Matrix Membranes Based on Metal−Organic Frameworks with Tunable Pore Size for CO_2 Separation

Lili Fan, Zixi Kang,* Yuting Shen, Sasa Wang, Haoru Zhao, Hanyi Sun, Xueting Hu, Haixiang Sun, Rongming Wang, and Daofeng Sun*

College of Science, China University of Petroleum (East China), Qingdao Shandong 266580, People's Republic of China

Supporting Information

ABSTRACT: Two isomorphous MOFs (Ni_2(L-asp)$_2$bipy and Ni_2(L-asp)$_2$pz) with different pore sizes were incorporated into poly(ether-*block*-amide) (Pebax-1657) to prepare the mixed matrix membranes (MMMs) with gas permeation properties for CO_2, H_2, N_2, and CH_4. Different loading ratios of MOFs with mass percentage from 10% to 30% were studied. Compared with the pure polymer membrane, the as-synthesized two series of MMMs showed improved CO_2 permeability and CO_2/H_2 selectivity. The highest CO_2 permeation property was achieved by Ni_2(L-asp)$_2$bipy@Pebax-20 of 120.2 barrers with an enhanced CO_2/H_2 selectivity of 32.88 compared with 55.85 barrers and 1.729 of the pure polymer membrane, respectively, which makes it a potential candidate for future applications in CO_2 capturing.

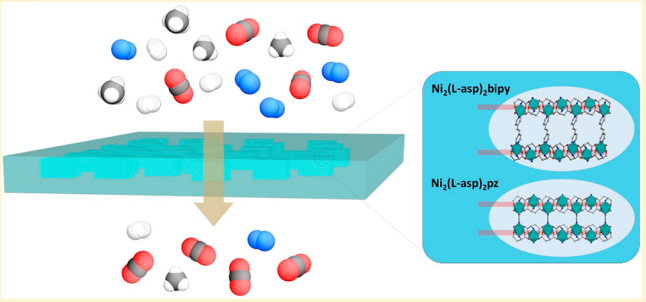

1. INTRODUCTION

The rising of population and explosive growth in energy consumption results in the enhancement of CO_2 content in the atmosphere, which probably causes a series of changes in human life.[1] CO_2 gas accounts for about 60% of the effect of greenhouse gases on global climate change.[2] To reduce CO_2 content, there are three main strategies, such as improving the efficiency of energy utilization, searching for new clean and renewable energy sources, and, more importantly, developing CO_2 capture technologies. Nowadays, both precombustion and postcombustion CO_2 captures need separation of CO_2 from other gas molecules.[2,3] Some technologies have been developed to capture and separate CO_2, including amine absorption process,[4,5] dual-alkali absorption approach,[6] molecular sieve adsorbent,[7,8] and cryogenic separation. However, most of these processes require high energy consumption to be carried out. Therefore, it is urgent to develop an alternative, cost-effective, and low energy consumption technology for CO_2 removal, such as membrane based separation.[9−12]

Membranes have been widely used in various industrial separations for the past decades.[9,13−16] Industrial applications are currently dominated by polymeric membranes.[17−20] Generally, advantages of using polymeric materials as membranes include: light weight, processability into different morphologies (such as thin films, porous beads, hollow fibers, and composites), and variations in structure and properties.[21] For polymer membrane based gas separation, a trade-off between selectivity and permeability usually appears, which is due to the nature of polymer materials.[22,23] To solve this issue, microporous fillers have been involved into the polymer matrix to form mixed matrix membranes (MMMs).[24−26] In the pioneering work, zeolites were used as fillers to combine with polymers to give improved gas separation performances compared with pure polymer membranes.[24] However, the weak interaction between inorganic filler and polymer phase usually leads to a rigidified interface or sieve-in-cage structure that holds back the performance enhancement of zeolite based MMMs. To this end, application of new microporous fillers that can improve the interaction with polymer phase is vital to the performance enhancement of the MMMs.

Metal−organic frameworks (MOFs) are a merging group of nanoporous materials constructed from inorganic metal centers and organic linkers, which have attracted great research interests in the fields of separation and adsorption due to their well-defined pores, large surface areas, and tunable pore sizes and chemical environment.[27−33] Recent experimental efforts have led to the conclusion that MOFs used as fillers are more compatible with polymers since MOFs possess organic linkers in the structure that can enhance the adhesion to polymer phase.[34−38] Furthermore, in the study reported by Long et al., MOF fillers can help polymers to overcome the issue of plasticization conversely.[39]

Due to the advantage of tunable pore sizes, in this work, we report on the design and fabrication of MMMs based on MOFs with different pore sizes for CO_2 capture application. A kind of commercial polyether block amide Pebax MH 1657 (Pebax) was used as the polymer matrix (Figure S1).[40−42] Two isomorphous MOF frameworks, Ni_2(L-asp)$_2$bipy and Ni_2(L-

Received: February 28, 2018
Revised: June 5, 2018
Published: June 15, 2018

DOI: 10.1021/acs.cgd.8b00307
Cryst. Growth Des. 2018, 18, 4365−4371

asp)$_2$pz (L-asp = L-aspartic acid, bipy = 4,4′-bipyridine, and pz = pyrazine), were chosen as fillers with a window size of 3.8 × 4.7 Å and 2.5 × 4.5 Å, respectively. The difference in pore size is brought by the different lengths of organic linker. These two MOFs were combined with Pebax polymer and made into MMMs with different loading amount.[12,43] The obtained MMMs were characterized by powder X-ray diffraction (PXRD), scanning electron microscope (SEM), thermogravimetric analysis (TGA), and Fourier transform infrared spectroscopy (FTIR). The gas permeability of MMMs was also tested, and the results showed that the introduction of Ni_2(L-asp)$_2$bipy and Ni_2(L-asp)$_2$pz improved the CO_2 permeability and CO_2/H_2 selectivity of the polymer membrane.

2. MATERIAL AND METHODS

2.1. Synthesis of MOF Crystals. Both Ni_2(L-asp)$_2$bipy and Ni_2(L-asp)$_2$pz crystals were synthesized by the conventional solvothermal method. First, $NiCO_3{\cdot}2Ni(OH)_2{\cdot}xH_2O$ (2.450 g) and L-aspartic acid (2.630 g) were dissolved in water (200 mL) under stirring and heating for 3 h. After filtering out all the remaining solid particles, the clear turquoise solution was then evaporated at 80 °C in an oven overnight to obtain the Ni(L-asp) powder. For the synthesis of Ni_2(L-asp)$_2$bipy MOF, a mixture of Ni(L-asp) (0.22 mmol), bipy (0.49 mmol), H_2O (6 mL), and methanol (6 mL) was sealed in the autoclave and heated in a 150 °C oven for 24 h. For the synthesis of Ni_2(L-asp)$_2$pz MOF, the same conditions were applied, while 4,4′-bipyridine was replaced by the same moles of pyrazine. The green MOFs powders were filtered and washed several times with a solution of water/methanol (1:1, v/v) to remove the unreacted reagents and then dried in a 60 °C oven.

2.2. Preparation of MMMs with Different Loading of MOFs Fillers. A certain amount of Ni_2(L-asp)$_2$bipy or Ni_2(L-asp)$_2$pz crystals were ground and dispersed in ethanol and water mixed solution with a mass ratio of 7:3, followed by sonication and stirring for 10 min, respectively. The obtained suspension was mixed with Pebax polymer and refluxed under 80 °C for 12 h. The loading amount of MOFs was varied from 10% to 30%, while the mass ratio of Pebax and solvent was 5:95. The final mixed solution was casted on a flat glass substrate. After the evaporation of ethanol and water in the air for 12 h and then in vacuum for 24 h at 40 °C, the prepared Ni_2(L-asp)$_2$bipy@Pebax-*x* and Ni_2(L-asp)$_2$pz@Pebax-*x* (where *x* represents the mass percentage of MOF fillers) were ripped off carefully from the glass substrate for characterization and gas permeability tests.

2.3. Characterizations. Information about the crystalline structure of the MOFs and MMMs was collected on a Bruker AXS D8 Advance instrument. The microscopic features of these membranes were characterized by a scanning electron microscope (JEOS JSM-6510A). The optical photos of the membranes were taken by a mobile phone at normal camera mode. The Fourier transform infrared spectroscopy (FTIR) spectra of membrane materials were collected by Spectrum One, and thermal gravimetric analysis on materials was carried out by a TGA/DSC1Mettler Toledo.

2.4. Gas Permeability Test. The MMMs were tested for their H_2, CO_2, N_2, and CH_4 pure gas permeation properties. Pure gas measurements were carried out using a variable pressure constant-volume gas permeation cell technique. The permeation cell setup and testing procedures had been described elsewhere.[1] The operating temperature was 35 °C, and the upstream gauge pressure was 1 atm. The gas permeability was calculated from the rate of pressure increasing (dp/dt) at a steady state according to the following eq 1

$$P = \frac{273 \times 10^{10}}{760} \frac{VL}{AT(p_2 \times 76/14.7)} \left(\frac{dp}{dt}\right) \quad (1)$$

where P is the membrane gas permeability in barrers (1 barrer = 1×10^{-10} cm^3(STP)·cm·cm^{-2}·s^{-1}·cmHg^{-1}), V represents the volume of the downstream reservoir (cm^3), A is the effective membrane area (cm^2), L refers to the membrane thickness (cm), T is the operating temperature (K), and p_2 indicates the upstream pressure (psia).

The ideal permselectivity was calculated based on the following eq 2:

$$\alpha(i/j) = \frac{P_i}{P_j} \quad (2)$$

3. RESULTS AND DISCUSSION

3.1. Membrane Characterizations. As shown in Figure 1, two isomorphous MOF frameworks Ni_2(L-asp)$_2$bipy and Ni_2(L-asp)$_2$pz with different pore sizes were used as fillers in this work. The structures of the MOF fillers and the corresponding MMMs with different MOF loading amounts were characterized by powder X-ray diffraction in the range from 4° to 40° (Figure 2). As can be seen, the diffraction peaks of the as-synthesized MOF fillers are in accordance with the simulated patterns, indicating their good crystallinity and phase purity. Though the pure polymer shows an amorphous structure with no obvious peaks, the typical features of the MOF fillers appear in the patterns of MOFs@Pebax MMMs as expected. The strong peak at a 2θ angle of 16.7° in Figure 2a is associated with the (1 1 0) crystal plane of Ni_2(L-asp)$_2$bipy, which indicates that the Ni_2(L-asp)$_2$bipy particles were incorporated in the membrane with a preferential crystal orientation. It may be an important factor determining the separation performance of the Ni_2(L-asp)$_2$bipy@Pebax MMMs. The intensity of the diffraction peaks in both series of MMMs becomes stronger when the loading amount of MOF fillers increases, which also indicates that the structure of MOF fillers is maintained well in the MMMs.

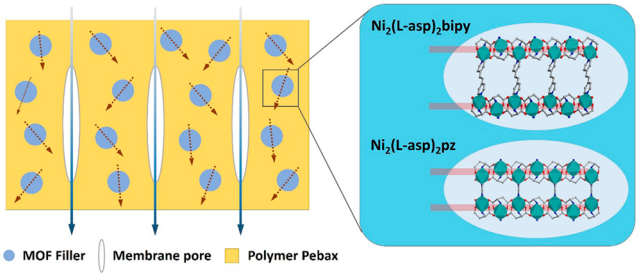

Figure 1. Schematic illustration of the MMMs structure and the possible gas transport mechanism.

The pure polymer Pebax membrane is colorless (Figure S2) and shows a smooth surface (Figure 3b). After incorporation of MOF fillers, as shown in the optical picture of membrane Ni_2(L-asp)$_2$bipy@Pebax-20 (Figure 3a), the membrane turns to light green and the surface becomes rough (Figure 3c). The membrane layer is composed of MOF particles and polymer, and the thickness of the membrane is determined to be 90–110 μm. Closer inspection of the respective MMM cross section reveals that there is macroscopic plastic deformation seen as polymer veins. It therefore suggests an even distribution of MOFs fillers in the polymer matrix. The formation of these veins is due to plastic deformation, which has also been seen in other MOF based MMMs and attributed to a strong interaction between the polymer and the fillers.[2] Other membranes with different MOF loading amounts were also characterized in the same manner, and the SEM images are shown in the Supporting Information (Figures S3 and S4).

DOI: 10.1021/acs.cgd.8b00307
Cryst. Growth Des. 2018, 18, 4365–4371

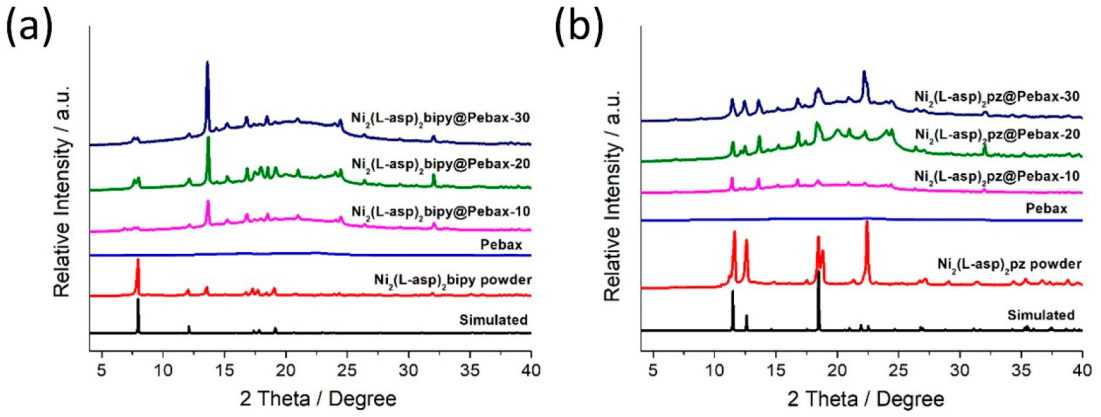

Figure 2. PXRD patterns of the simulated and as-synthesized MOF fillers, pure polymer Pebax, and the corresponding MMMs with different loading amounts of MOF fillers.

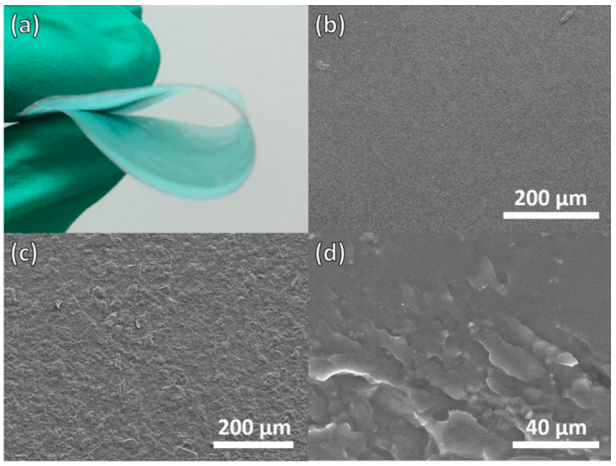

Figure 3. (a) Optical image of membrane Ni_2(L-asp)$_2$bipy@Pebax-20. SEM images of (b) the pure polymer Pebax membrane, (c) the top view and (d) cross section of membrane Ni_2(L-asp)$_2$bipy@Pebax-20.

The structural stability and integrity of MOF fillers and the MMMs were studied by TGA (Figure 4a,b). The slight weight loss of the Ni_2(L-asp)$_2$bipy and Ni_2(L-asp)$_2$pz powders from 100 to 200 °C can be attributed to the removal of absorbed water. Both of the MOF fillers exhibit a decomposition temperature above 350 °C, which has even been increased to around 400 °C after incorporated in the Pebax polymer due to the strong interaction between the MOF fillers and the polymer matrix. These results prove that the as-synthesized MMMs are quite stable for industrial application such as gas separation. FTIR tests were also carried out on the pure polymer membrane and the MMMs (Figure 4c,d). For the pure polymer membrane, the peaks of 1100 and 1640 cm^{-1} are referred to the ester groups, while the peaks of 1545 and 3300 cm^{-1} can be assigned to the methylene and amine of the Pebax, respectively. Compared with the pure polymer membrane, new peaks of 865, 1422, and 1576 cm^{-1} are detected according to the organic ligands of MOF fillers, which further proves the successful incorporation of MOF fillers in the Pebax polymer.

3.2. Gas Permeability. Single gas permeation experiments of H_2, N_2, CO_2, and CH_4 for the pure polymer membrane and the two series of MOFs@Pebax MMMs were carried out, and the results are summarized in Figure 5 and Tables S1 and S2. It can be seen that the presence of MOFs strongly affects the gas transport properties of the membranes. For the membranes using Ni_2(L-asp)$_2$bipy as the filler (Figure 5a), the CO_2 permeability increases significantly compared with the pure polymer, and the highest permeability is obtained when the loading amount reaches 20%. The membrane of Ni_2(L-asp)$_2$bipy@Pebax-20 possesses permeability around 120 barrers, which is twice as much as that of the pure polymer. The enhancement of permeability can be attributed to strong affinity for CO_2 molecules of the Ni_2(L-asp)$_2$bipy structure, which facilitates their diffusion and thus enhances the permeability. The reduced crystallization and free volume introduced by incorporation of Ni_2(L-asp)$_2$bipy also make the transport of CO_2 easier through the membrane.[44] When the loading amount of Ni_2(L-asp)$_2$bipy increases to 30%, a decrease of CO_2 permeability appears for some degree of membrane inhomogeneity brought by preparation difficulty, which limits the effect of the MOF fillers.

As shown in Figure 5a, the permeability of H_2 is obviously suppressed by Ni_2(L-asp)$_2$bipy incorporation and changes slightly with the increase of the filler loading amount. That is because the Ni_2(L-asp)$_2$bipy particles present a preferential crystal orientation in the membrane certified by XRD results. Along the [1 1 0] direction, there are no structural pores (Figure S5b) and the transport of H_2 molecules is blocked, which thus decreases the H_2 permeability. Basing on the sorption-diffusion mechanism, it is different from CO_2 for the reason that CO_2 can be strongly adsorbed by the Ni_2(L-asp)$_2$bipy framework pores from other directions. The permeability of N_2 and CH_4 changes not much due to the larger kinetic diameter of N_2 (3.6 Å) and CH_4 (3.8 Å) compared to CO_2 (3.3 Å). Corresponding ideal selectivities are calculated based on the permeance results (Figure 5c). Compared with the pure polymer membrane, the CO_2/H_2 selectivity of Ni_2(L-asp)$_2$bipy@Pebax-20 is greatly enhanced to 32.88 from 1.73, surpassing many of the reported membranes (Table S4), while the CO_2/N_2 selectivity is increased to 52 under 30% loading amount and the CO_2/CH_4 selectivity is well held when the loading amount reached 20% and 30%, respectively. Binary gas mixture (CO_2/H_2, CO_2/N_2, and CO_2/CH_4) permeation properties were further investigated on Ni_2(L-asp)$_2$bipy@Pebax-20 membrane, and similar separation performances were obtained (Figure S6 and Table S3). The permeability of CO_2 is a little lower than the single gas tests due to the blocking effect brought by the other kind of gas

DOI: 10.1021/acs.cgd.8b00307
Cryst. Growth Des. 2018, 18, 4365−4371

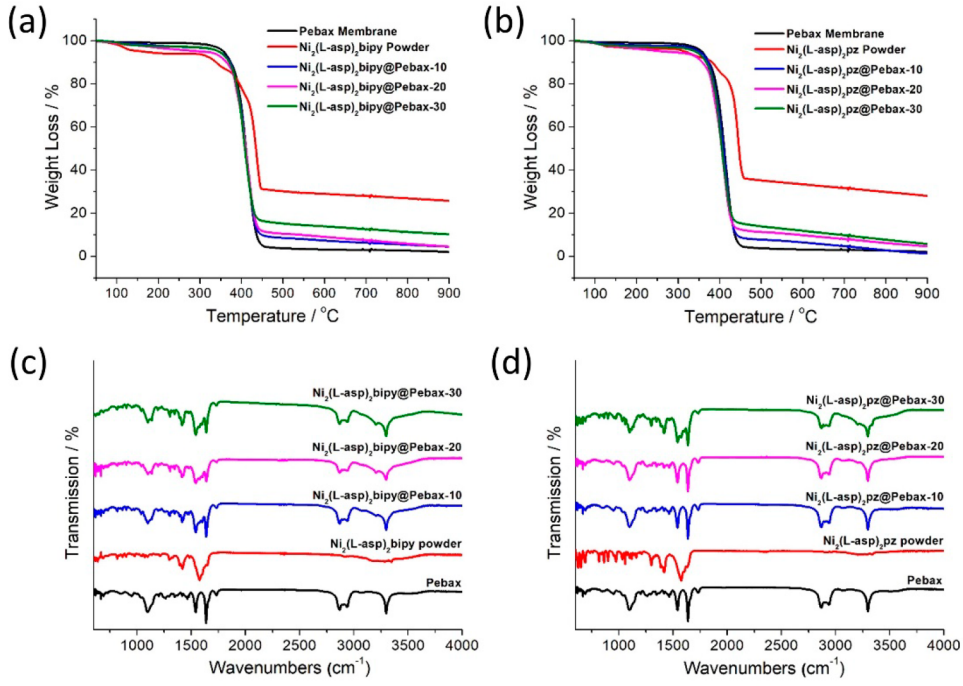

Figure 4. TGA curves of the two MOF fillers (a) Ni_2(L-asp)$_2$bipy and (b) Ni_2(L-asp)$_2$pz based MMMs. Corresponding FTIR spectra of (c) Ni_2(L-asp)$_2$bipy and (d) Ni_2(L-asp)$_2$pz based MMMs.

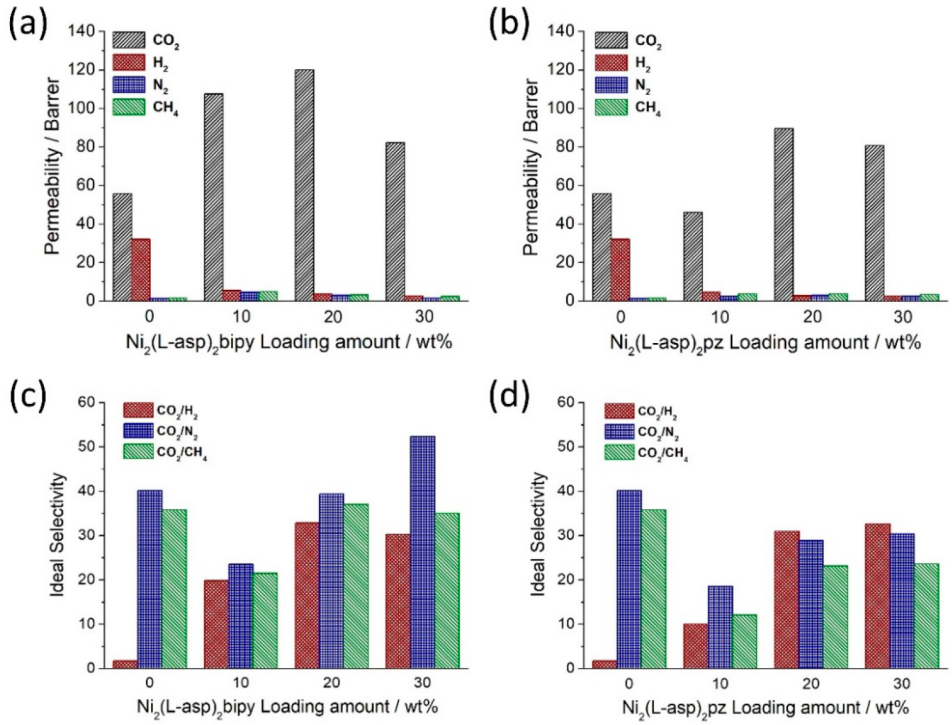

Figure 5. Single gas permeability of the two MOF fillers (a) Ni_2(L-asp)$_2$bipy and (b) Ni_2(L-asp)$_2$pz based MMMs. Corresponding ideal selectivity of (c) Ni_2(L-asp)$_2$bipy and (d) Ni_2(L-asp)$_2$pz based MMMs.

molecules, which contributes to the slight reduction of CO_2/H_2, CO_2/N_2, and CO_2/CH_4 selectivity.

In the case of Ni_2(L-asp)$_2$pz as the filler, the CO_2 permeability is not increased as high as the Ni_2(L-asp)$_2$bipy based membranes and even declined when the loading amount was 10%. This is mainly due to the more effective sieving effect played by the small window size of Ni_2(L-asp)$_2$pz. The kinetic diameter of CO_2 is larger than the window size; however, they still can be adsorbed by the Ni_2(L-asp)$_2$pz framework owing to its flexibility. The transport of CO_2 is constrained to some extent, resulting in reduced permeability than that of Ni_2(L-asp)$_2$bipy based membranes. Without the special affinity, even smaller as H_2 cannot enter and move freely in the pores of Ni_2(L-asp)$_2$pz in the MMM. So it is harder for N_2 and CH_4

DOI: 10.1021/acs.cgd.8b00307
Cryst. Growth Des. 2018, 18, 4365−4371

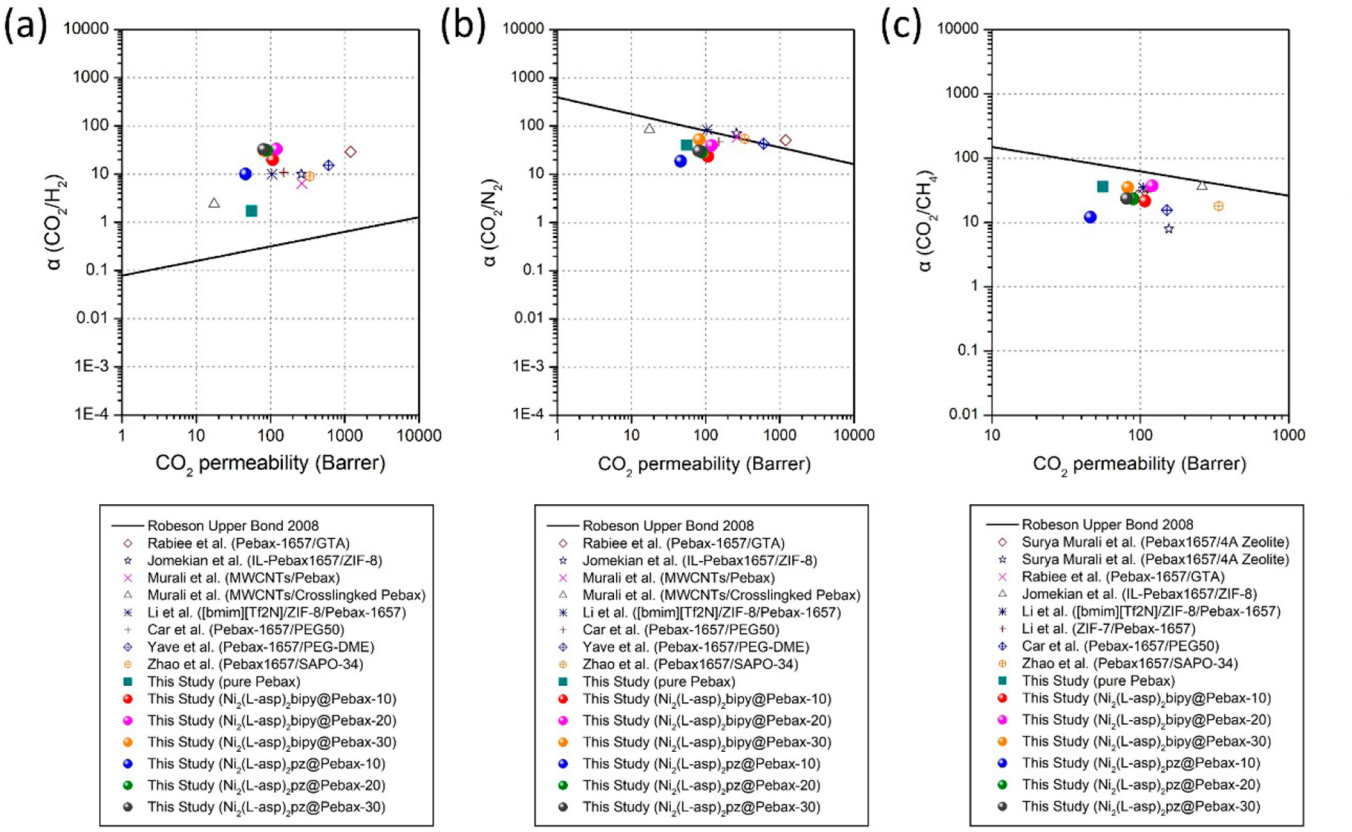

Figure 6. Comparison of (a) CO_2/H_2, (b) CO_2/N_2, and (c) CO_2/CH_4 separation performance of the as-synthesized and reported MMMs based on MOFs with Robeson's upper bound line (data selected from Tables S1, S2, and S4).[9,45−52]

with larger kinetic diameters. The permeability fluctuations of H_2, N_2, and CH_4 with varied Ni_2(L-asp)$_2$pz loading amounts are mainly caused by the free volume introduced after MOF incorporation. Accordingly, degraded ideal selectivities of CO_2/H_2, CO_2/N_2, and CO_2/CH_4 are detected for nearly all the Ni_2(L-asp)$_2$pz@Pebax MMMs.

The separation performances of the pure Pebax membrane, the Ni_2(L-asp)$_2$bipy and Ni_2(L-asp)$_2$pz based MMMs were also compared with the well-known Robeson upper bound. As shown in Figure 6, the two MOF fillers offer substantial improvement in CO_2 permeability (increased by 115% for Ni_2(L-asp)$_2$bipy@Pebax-20 and 60.5% for Ni_2(L-asp)$_2$pz@Pebax-20) over the pure Pebax membrane. Compared with other reported MOF-based MMMs, the membranes fabricated in this work exhibited well-balanced performance with higher CO_2/H_2 selectivity and intermediate permeability. More importantly, the comparison of the results of these two series of MMMs proves that the tunable pore sizes of the fillers play an important role in regulating the membrane properties, including the permeability and selectivity. The Ni_2(L-asp)$_2$bipy MOF with larger pore size can provide additional fractional free volume for gas diffusion, resulting in increased diffusion coefficient; thus, the CO_2 permeability of Ni_2(L-asp)$_2$bipy@Pebax-20 is greatly improved compared with the pristine Pebax membrane. On the other hand, the window of Ni_2(L-asp)$_2$pz is too small to let CO_2 molecules pass through, leading to the lower increase of CO_2 permeability for Ni_2(L-asp)$_2$pz@Pebax MMMs. The different sieving effects brought by fillers with different pore sizes may be an important point to be considered in future MMMs fabrication.

4. CONCLUSIONS

In summary, Pebax was chosen as the matrix to prepare mixed matrix membranes via incorporation of two isomorphous MOFs with different pore sizes. The loading ratio was varied from 10% to 30%. PXRD, SEM, FTIR, and TGA tests were carried out to characterize the structure, morphology, and stability of the obtained membranes. For the gas transport property, MOFs based membranes show improved CO_2 permeability and CO_2/H_2 selectivity compared with the pure polymer membrane. Ni_2(L-asp)$_2$bipy@Pebax-20 exhibits a CO_2 permeability of 120.2 barrers with an enhanced CO_2/H_2 selectivity of 32.88 contrasted with 55.85 barrers and 1.729 of the pure membrane, which surpasses many of the reported membranes. These performances make the MMMs prepared in this work potential candidates for applications in capturing CO_2.

■ ASSOCIATED CONTENT

Supporting Information

The Supporting Information is available free of charge on the ACS Publications website at DOI: 10.1021/acs.cgd.8b00307.

Details for structural formula of Pebax polymer, optical image of pure Pebax membrane, SEM images of the MMMs, 3D structure of Ni_2(L-asp)$_2$bipy, gas separation data of this work, and comparison with other reported work (PDF)

■ AUTHOR INFORMATION

Corresponding Authors

*E-mail: kangzixi69@126.com (Z.K.).

DOI: 10.1021/acs.cgd.8b00307
Cryst. Growth Des. 2018, 18, 4365−4371

*E-mail: dfsun@upc.edu.cn (D.S.).

ORCID

Rongming Wang: 0000-0002-5445-541X
Daofeng Sun: 0000-0003-3184-1841

Author Contributions

The manuscript was written through contributions of all authors. All authors have given approval to the final version of the manuscript.

Notes

The authors declare no competing financial interest.

■ ACKNOWLEDGMENTS

This work was supported by the National Natural Science Foundation of China (Grant Nos. 21571187, 21501198, 21601205), Taishan Scholar Foundation (ts201511019), and the Fundamental Research Funds for the Central Universities (18CX02047A, 18CX07001A).

■ ABBREVIATIONS

MMMs, mixed matrix membranes; MOFs, metal−organic frameworks

■ REFERENCES

(1) Yang, H.; Xu, Z.; Fan, M.; Gupta, R.; Slimane, R. B.; Bland, A. E.; Wright, I. Progress in carbon dioxide separation and capture: A review. *J. Environ. Sci.* **2008**, *20*, 14−27.
(2) Lin, W. H.; Vora, R. H.; Chung, T. S. Gas transport properties of 6FDA-durene/1,4-phenylenediamine (pPDA) copolyimides. *J. Polym. Sci., Part B: Polym. Phys.* **2000**, *38*, 2703−2713.
(3) Kang, Z.; Peng, Y.; Hu, Z.; Qian, Y.; Chi, C.; Yeo, L. Y.; Tee, L.; Zhao, D. Mixed matrix membranes composed of two-dimensional metal−organic framework nanosheets for pre-combustion CO_2 capture: a relationship study of filler morphology versus membrane performance. *J. Mater. Chem. A* **2015**, *3*, 20801−20810.
(4) Jabbari, V.; Veleta, J. M.; Zarei-Chaleshtori, M.; Gardea-Torresdey, J.; Villagrán, D. Green synthesis of magnetic MOF@GO and MOF@CNT hybrid nanocomposites with high adsorption capacity towards organic pollutants. *Chem. Eng. J.* **2016**, *304*, 774−783.
(5) Yan, J.; Yu, Y.; Xiao, J.; Li, Y.; Li, Z. Improved Ethanol Adsorption Capacity and Coefficient of Performance for Adsorption Chillers of Cu-BTC@GO Composite Prepared by Rapid Room Temperature Synthesis. *Ind. Eng. Chem. Res.* **2016**, *55*, 11767−11774.
(6) Huang, H. P.; Shi, Y.; Li, W.; Chang, S. G. Dual alkali approaches for the capture and separation. *Energy Fuels* **2001**, *15*, 263−268.
(7) Ho, M. T.; Allinson, G. W.; Wiley, D. E. Reducing the cost of CO_2 capture from flue gases using pressure swing adsorption. *Ind. Eng. Chem. Res.* **2008**, *47*, 4883−4890.
(8) Liu, J.; Thallapally, P. K.; McGrail, B. P.; Brown, D. R.; Liu, J. Progress in adsorption-based CO_2 capture by metal-organic frameworks. *Chem. Soc. Rev.* **2012**, *41*, 2308−2322.
(9) Zhao, D.; Ren, J.; Li, H.; Hua, K.; Deng, M. Poly(amide-6-b-ethylene oxide)/SAPO-34 mixed matrix membrane for CO_2 separation. *J. Energy Chem.* **2014**, *23*, 227−234.
(10) Pera-Titus, M. Porous Inorganic Membranes for CO_2 Capture: Present and Prospects. *Chem. Rev.* **2014**, *114*, 1413−1492.
(11) Ramasubramanian, K.; Zhao, Y.; Winston Ho, W. S. CO_2capture and H_2 purification: Prospects for CO_2-selective membrane processes. *AIChE J.* **2013**, *59*, 1033−1045.
(12) Kang, Z.; Xue, M.; Fan, L.; Huang, L.; Guo, L.; Wei, G.; Chen, B.; Qiu, S. Highly selective sieving of small gas molecules by using an ultra-microporous metal−organic framework membrane. *Energy Environ. Sci.* **2014**, *7*, 4053−4060.
(13) Caro, J. Are MOF membranes better in gas separation than those made of zeolites? *Curr. Opin. Chem. Eng.* **2011**, *1*, 77−83.
(14) Gascon, J.; Kapteijn, F. Metal-organic framework membranes−high potential, bright future? *Angew. Chem., Int. Ed.* **2010**, *49*, 1530−2.
(15) Li, Y.; Yang, W. Microwave synthesis of zeolite membranes: A review. *J. Membr. Sci.* **2008**, *316*, 3−17.
(16) Baker, R. W. Future directions of membrane gas separation technology. *Ind. Eng. Chem. Res.* **2002**, *41*, 1393−1411.
(17) Lin, H. Q.; Van Wagner, E.; Raharjo, R.; Freeman, B. D.; Roman, I. High-performance polymer membranes for natural-gas sweetening. *Adv. Mater.* **2006**, *18*, 39−44.
(18) Carta, M.; Malpass-Evans, R.; Croad, M.; Rogan, Y.; Jansen, J. C.; Bernardo, P.; Bazzarelli, F.; McKeown, N. B. An efficient polymer molecular sieve for membrane gas separations. *Science* **2013**, *339*, 303−7.
(19) Shao, P.; Huang, R. Y. M. Polymeric membrane pervaporation. *J. Membr. Sci.* **2007**, *287*, 162−179.
(20) Feng, C. Y.; Khulbe, K. C.; Matsuura, T.; Ismail, A. F. Recent progresses in polymeric hollow fiber membrane preparation, characterization and applications. *Sep. Purif. Technol.* **2013**, *111*, 43−71.
(21) Zhang, C.; Zhang, K.; Xu, L.; Labreche, Y.; Kraftschik, B.; Koros, W. J. Highly scalable ZIF-based mixed-matrix hollow fiber membranes for advanced hydrocarbon separations. *AIChE J.* **2014**, *60*, 2625−2635.
(22) Freeman, B. D. Basis of Permeability/Selectivity Tradeoff Relations in Polymeric Gas Separation Membranes. *Macromolecules* **1999**, *32*, 375−380.
(23) Robeson, L. M. The upper bound revisited. *J. Membr. Sci.* **2008**, *320*, 390−400.
(24) Chung, T.-S.; Jiang, L. Y.; Li, Y.; Kulprathipanja, S. Mixed matrix membranes (MMMs) comprising organic polymers with dispersed inorganic fillers for gas separation. *Prog. Polym. Sci.* **2007**, *32*, 483−507.
(25) Li, S.; Falconer, J. L.; Noble, R. D. Improved SAPO-34 membranes for CO_2/CH_4 separations. *Adv. Mater.* **2006**, *18*, 2601−2603.
(26) Hinds, B. J.; Chopra, N.; Rantell, T.; Andrews, R.; Gavalas, V.; Bachas, L. G. Aligned multiwalled carbon nanotube membranes. *Science* **2004**, *303*, 62−65.
(27) Furukawa, H.; Cordova, K. E.; O'Keeffe, M.; Yaghi, O. M. The Chemistry and Applications of Metal-Organic Frameworks. *Science* **2013**, *341*, 1230444.
(28) Cui, X.; Chen, K.; Xing, H.; Yang, Q.; Krishna, R.; Bao, Z.; Wu, H.; Zhou, W.; Dong, X.; Han, Y.; Li, B.; Ren, Q.; Zaworotko, M. J.; Chen, B. Pore chemistry and size control in hybrid porous materials for acetylene capture from ethylene. *Science* **2016**, *353*, 141−144.
(29) Cadiau, A.; Adil, K.; Bhatt, P. M.; Belmabkhout, Y.; Eddaoudi, M. A metal-organic framework-based splitter for separating propylene from propane. *Science* **2016**, *353*, 137−140.
(30) Kang, Z.; Fan, L.; Wang, S.; Sun, D.; Xue, M.; Qiu, S. In situ confinement of free linkers within a stable MOF membrane for highly improved gas separation properties. *CrystEngComm* **2017**, *19*, 1601−1606.
(31) Liang, L.; Liu, C.; Jiang, F.; Chen, Q.; Zhang, L.; Xue, H.; Jiang, H.-L.; Qian, J.; Yuan, D.; Hong, M. Carbon dioxide capture and conversion by an acid-base resistant metal-organic framework. *Nat. Commun.* **2017**, *8*, 1233.
(32) Yang, Y.; Jiang, F.; Chen, L.; Pang, J.; Wu, M.; Wan, X.; Pan, J.; Qian, J.; Hong, M. An unusual bifunctional Tb-MOF for highly sensitive sensing of Ba^{2+} ions and with remarkable selectivities for CO_2-N_2 and CO_2-CH_4. *J. Mater. Chem. A* **2015**, *3*, 13526−13532.
(33) Gu, Z.-G.; Zhang, J. Epitaxial growth and applications of oriented metal-organic framework thin films. *Coord. Chem. Rev.* **2017**, DOI: 10.1016/j.ccr.2017.09.028.
(34) Zhang, C.; Dai, Y.; Johnson, J. R.; Karvan, O.; Koros, W. J. High performance ZIF-8/6FDA-DAM mixed matrix membrane for propylene/propane separations. *J. Membr. Sci.* **2012**, *389*, 34−42.

DOI: 10.1021/acs.cgd.8b00307
Cryst. Growth Des. 2018, 18, 4365−4371

(35) Thompson, J. A.; Chapman, K. W.; Koros, W. J.; Jones, C. W.; Nair, S. Sonication-induced Ostwald ripening of ZIF-8 nanoparticles and formation of ZIF-8/polymer composite membranes. *Microporous Mesoporous Mater.* **2012**, *158*, 292−299.
(36) Dai, Y.; Johnson, J. R.; Karvan, O.; Sholl, D. S.; Koros, W. J. Ultem((R))/ZIF-8 mixed matrix hollow fiber membranes for CO_2/N_2 separations. *J. Membr. Sci.* **2012**, *401*−*402*, 76−82.
(37) Rodenas, T.; Luz, I.; Prieto, G.; Seoane, B.; Miro, H.; Corma, A.; Kapteijn, F.; Llabres i Xamena, F. X.; Gascon, J. Metal-organic framework nanosheets in polymer composite materials for gas separation. *Nat. Mater.* **2015**, *14*, 48−55.
(38) Erucar, I.; Yilmaz, G.; Keskin, S. Recent advances in metal-organic framework-based mixed matrix membranes. *Chem. - Asian J.* **2013**, *8*, 1692−704.
(39) Bachman, J. E.; Smith, Z. P.; Li, T.; Xu, T.; Long, J. R. Enhanced ethylene separation and plasticization resistance in polymer membranes incorporating metal-organic framework nanocrystals. *Nat. Mater.* **2016**, *15*, 845−849.
(40) Ren, X.; Ren, J.; Li, H.; Feng, S.; Deng, M. Poly (amide-6-b-ethylene oxide) multilayer composite membrane for carbon dioxide separation. *Int. J. Greenhouse Gas Control* **2012**, *8*, 111−120.
(41) Kaneti, Y. V.; Tang, J.; Salunkhe, R. R.; Jiang, X.; Yu, A.; Wu, K. C.; Yamauchi, Y. Nanoarchitectured Design of Porous Materials and Nanocomposites from Metal-Organic Frameworks. *Adv. Mater.* **2017**, *29*, 1604898.
(42) Wang, L.; Han, Y.; Feng, X.; Zhou, J.; Qi, P.; Wang, B. Metal−organic frameworks for energy storage: Batteries and supercapacitors. *Coord. Chem. Rev.* **2016**, *307*, 361−381.
(43) Vaidhyanathan, R.; Bradshaw, D.; Rebilly, J.-N.; Barrio, J. P.; Gould, J. A.; Berry, N. G.; Rosseinsky, M. J. A Family of Nanoporous Materials Based on an Amino Acid Backbone. *Angew. Chem.* **2006**, *118*, 6645−6649.
(44) Azizi, N.; Mohammadi, T.; Behbahani, R. M. Synthesis of a PEBAX-1074/ZnO nanocomposite membrane with improved CO_2 separation performance. *J. Energy Chem.* **2017**, *26*, 454−465.
(45) Surya Murali, R.; Ismail, A. F.; Rahman, M. A.; Sridhar, S. Mixed matrix membranes of Pebax-1657 loaded with 4A zeolite for gaseous separations. *Sep. Purif. Technol.* **2014**, *129*, 1−8.
(46) Rabiee, H.; Soltanieh, M.; Mousavi, S. A.; Ghadimi, A. Improvement in CO_2/H_2 separation by fabrication of poly(ether-b-amide6)/glycerol triacetate gel membranes. *J. Membr. Sci.* **2014**, *469*, 43−58.
(47) Jomekian, A.; Bazooyar, B.; Behbahani, R. M.; Mohammadi, T.; Kargari, A. Ionic liquid-modified Pebax® 1657 membrane filled by ZIF-8 particles for separation of CO_2 from CH_4, N_2 and H_2. *J. Membr. Sci.* **2017**, *524*, 652−662.
(48) Murali, R. S.; Sridhar, S.; Sankarshana, T.; Ravikumar, Y. V. L. Gas Permeation Behavior of Pebax-1657 Nanocomposite Membrane Incorporated with Multiwalled Carbon Nanotubes. *Ind. Eng. Chem. Res.* **2010**, *49*, 6530−6538.
(49) Li, H.; Tuo, L.; Yang, K.; Jeong, H.-K.; Dai, Y.; He, G.; Zhao, W. Simultaneous enhancement of mechanical properties and CO_2 selectivity of ZIF-8 mixed matrix membranes: Interfacial toughening effect of ionic liquid. *J. Membr. Sci.* **2016**, *511*, 130−142.
(50) Li, T.; Pan, Y.; Peinemann, K.-V.; Lai, Z. Carbon dioxide selective mixed matrix composite membrane containing ZIF-7 nano-fillers. *J. Membr. Sci.* **2013**, *425*, 235−242.
(51) Car, A.; Stropnik, C.; Yave, W.; Peinemann, K.-V. PEG modified poly(amide-b-ethylene oxide) membranes for CO_2 separation. *J. Membr. Sci.* **2008**, *307*, 88−95.
(52) Yave, W.; Car, A.; Peinemann, K.-V. Nanostructured membrane material designed for carbon dioxide separation. *J. Membr. Sci.* **2010**, *350*, 124−129.

DOI: 10.1021/acs.cgd.8b00307
Cryst. Growth Des. 2018, 18, 4365−4371